N71-28968
NASA TM X-67861

NASA TECHNICAL MEMORANDUM

NASA TM X-67861

MEASURED AND CALCULATED FAST NEUTRON SPECTRA IN A LEAD-AND-WATER SHIELDED REACTOR

by Gerald P. Lahti and Gilbert N. Wrights
Lewis Research Center
Cleveland, Ohio

TECHNICAL PAPER proposed for presentation at
American Nuclear Society National Meeting
Boston, Massachusetts, June 13-17, 1971

ABSTRACT

Measurements of neutron spectra were made in a cylindrical shield arrangement surrounding a small (25.4 cm diam) cylindrical UO_2F_2 - water solution reactor. The shield consisted of cylindrical shells of lead and water. The outside diameter of the shield was 244 cm. Measurements were made with a NE-213 scintillation spectrometer to depths into the shield of 100 cm. Calculations of absolute neutron flux spectra made with the two dimensional discrete ordinates code, DOT, agreed reasonably well with experiment. Calculations made with the one-dimensional discrete ordinates code ANISN diverged from the DOT results at deeper penetrations due to transverse leakage approximations. Sensitivity to neutron energy group structure was also investigated.

E-6394

MEASURED AND CALCULATED FAST NEUTRON SPECTRA IN A LEAD-AND-WATER SHIELDED REACTOR

by Gerald P. Lahti and Gilbert N. Wrights

National Aeronautics and Space Administration
Lewis Research Center
Cleveland, Ohio

SUMMARY

Measurements of absolute neutron flux spectra were made in a layered cylindrical shield arrangement surrounding a small (25.4 cm diam) cylindrical UO_2F_2 - water solution reactor. The shield consisted of 91.4 cm high cylindrical shells of lead and water and extended to an outer radius of 122 cm. Measurements were made within the shield to depths into the shield of up to 100 cm. Measurements were made with a 4.65 cm diameter by 4.38 cm high NE-213 liquid scintillator immersed in the water regions of the shield. The midplane of the detector was located along the midplane of the reactor. The pulse height distribution of the detector was unfolded using the FERDOR code.

Calculations of absolute neutron flux spectra for this geometry were made using the one-dimensional discrete ordinates code ANISN and the two-dimensional discrete ordinates code DOT. Preliminary calculations were made with ANISN to compare the adequacy of a coarse energy group split that was used in subsequent ANISN and DOT calculations. ANISN and DOT calculations were made with identical cross sections and radial geometry.

Comparison of these two calculations showed the depths in the shield at which ANISN and DOT results diverged as a result of transverse leakage approximations in ANISN. This point occurred at a radius of approximately 50 cm. Beyond this depth more confidence was placed in the DOT - calculated spectra.

TM X-67861

The DOT-calculated spectra are in reasonable agreement in both shape and magnitude with the measurement. There is a consistent difference in spectral shape however; namely that the measured spectra was greater than that calculated for neutron energies below 4 MeV, and vice versa for neutrons above 4 MeV. The spectra show the expected hardening with depth of penetration.

INTRODUCTION

The design of a minimum weight shield for a space power nuclear reactor requires confidence in calculations and cross section data. To check neutron transport calculations, a series of experiments is being conducted using the NASA Lewis zero power solution reactor (100 W thermal, maximum) and shield facility. The series of experiments is planned to examine, first, geometrically-clean configurations of materials for which neutron cross sections are well known, then geometrically-clean configurations of candidate space-power-reactor shielding materials, and finally the effect of shield perturbations such as ducts associated with a SNAP-8 reactor shield. The purpose of the clean-geometry experiments with materials for which neutron cross sections are well known is to test computation and measurement techniques before long-lead-time space power reactor shield materials can be obtained. Later clean-geometry experiments conducted with candidate shield materials could then perhaps reveal cross section uncertainties.

The present report describes calculations and measurements made for a cylindrical reactor surrounded by alternate layers of lead and water. Calculations were made using state-of-the-art methods, namely the one-dimensional S_n transport code ANISN (ref. 1) the two-dimensional S_n transport code DOT (refs. 2 and 3) and fast neutron cross sections from the GAM II (ref. 4) library. Measurements were made using state-of-the-art scintillator techniques developed mainly at Oak Ridge National Laboratory (refs. 5 and 6).

GEOMETRY OF EXPERIMENT

The test facility used in these experiments is the NASA Zero Power Reactor Facility. The uranyl fluoride solution reactor in this facility is 25.4 cm in diameter and, depending on fuel concentration and reflector material, can be operated at up to 76 cm in height. This reactor is licensed to operate at a maximum of 100 watts thermal (a total neutron source strength of about 8×10^{12} N/sec). The reactor vessel is 0.278 cm thick made of type 316 stainless steel. The reactor is surrounded by a 244 cm diameter by 104 cm deep cylindrical tank; shielding materials and/or configurations may be constructed in or about this large tank.

Additional shielding around the facility was installed to minimize room background. This shielding includes borated polyethylene slabs placed around the outside of the tank and borated polyethylene plugs placed at the top and bottom of the cylindrical reactor. These plugs reduce the rate of return of room-scattered neutrons and gamma rays as well as the rate of generation of gammas in the room due to neutron capture.

The present experimental configuration is illustrated in figure 1. The reactor is operated with a solution corresponding to hydrogen-to-uranium-235 ratio of 641. The reactor is surrounded by a cylindrical shell of 20.3 cm thick lead brick. The purpose of the lead is to substantially reduce the number of gamma rays leaking from the reactor core without substantially reducing the neutron leakage. This is necessary to minimize the difficulty in separating neutrons from gamma rays in the spectrometer system and also to permit one to collect more neutron information per unit time. For this experiment, the remainder of the tank is filled with water. Measurements of neutron spectra were taken at several positions in the water with and without a 5- or 10-cm thick intermediate lead wall located 64.5 cm from the vertical centerline of the core (see fig. 1).

For the case with no intermediate lead, measurements were made on the horizontal midplane with the center of the detector at 54.3, 77.1 and 100 cm from the vertical centerline of the core. For the cases with the intermediate lead wall in place, measurements were made at the 100 cm position with the 5 cm wall, and at 79.6 and 100 cm with the 10 cm wall.

NEUTRON SPECTRUM MEASUREMENTS

Spectrometer

Measurements were made using state-of-the-art liquid scintillator techniques developed mainly at Oak Ridge National Laboratory. A 4.38 by 4.65 centimeter diameter NE-213 liquid scintillator mounted on an RCA 8575 photomultiplier tube was used to measure neutron spectra. A block diagram of the spectrometer is shown in figure 2 along with the photomultiplier tube base circuit. A linear pulse is taken from the 10th dynode of the photomultiplier tube, amplified and sent to one side of the analyzer. The output of the modified Owen's pulse shape discriminator circuit is amplified and sent to the other side of the analyzer. Commercially available amplifiers and analyzer are used.

The proton recoil and compton electron recoil spectra were measured at two gain settings in the ratio of approximately 7-1/2 to 1. The photomultiplier tube was operated at 2050V for neutrons with energies less than 3 MeV, and at 1600V for neutrons with energies greater than 3 MeV. The detector was calibrated at both 2050 and 1600V using a Na^{22} gamma ray source.

The FERDOR code and the ORNL response functions for a 4.60 by 4.65 centimeter diameter scintillator were used to unfold the measured proton-recoil distributions. To permit use of the ORNL response functions, the proton-recoil count rates were increased by 5 percent to account for the shorter length of the NE-213 scintillator.

The uncertainty in the experimental measurements is determined by the counting statistics, the inherent uncertainty in the unfolding process, the estimated error in the response functions used for the spectrometer, and the uncertainty in the determination of the power level. The statistical and unfolding uncertainty are included in the FERDOR method of unfolding in which the upper and lower confidence limits of the unfolded spectra

encompass the true answer with a 68 percent probability. The response function error, resulting from the use of the detector in a flux field whose neutron angular distribution is not quite parallel and incident totally on the curved surface of the scintillator, is difficult to determine. Some idea of the response function error was obtained at an earlier date (ref. 7) by measuring a PuBe spectrum incident on the curved surface and then on the flat surface of the scintillator. These measurements showed no differences for neutron energies above 2 MeV, and differences of the order of 15 percent too low for neutron energies below 2 MeV when incident on the flat surface of the scintillator. The uncertainty in the absolute power level (discussed later) was estimated to be ±10 percent. Thus the measured spectra should be accurate to ±10 percent with the exception of the data below 2 MeV, which could be low by 15 percent depending upon the angular distribution of the flux. The unfolded data (fig. 6) is plotted as a vertical bar, representing the upper and lower confidence limits. Points indicate the average value. For data points having small error, the circles encompass the upper and lower limit. Counting times for one gain setting varied from 2 to 12 hours for the various amplifier gain settings used. Reactor power levels were of the order of 0.002 to 1.5 watts.

Location of Effective Center of Detection

The NE-213 detector used was 4.65 cm in diameter by 4.38 cm long. The flat end of the detector was attached to the flat end of a photomultiplier tube and wrapped with Al foil. The detector-photomultiplier tube-tube base assumbly was then placed in a 9.38 cm o.d. by 60 cm long by 0.16 cm thick Al container open at one end. The container, lined with a layer of lead 0.32 cm thick to reduce low energy gamma flux at the detector, was then suspended vertically in the water tank to make the measurements (see fig. 3). The axis of the scintillator, when operated, was vertical. The horizontal midplane of the scintillator, when operated, was located on the horizontal midplane of the reactor.

Because the detector volume is finite in size there is a question of the location of its effective center of detection; i.e., which radial point value in the calculation should be compared with experiment? Because of the highly forward anisotropy of the MeV neutrons at relatively deep penetrations; i.e., in radial directions away from the source region, and the large fall off of scalar flux across the diameter of the container it may be argued that the neutrons arrive predominantly from the front face of the detector container. The detector volume then sees, principally an anisotropic current of neutrons directed radially outward and arriving uncollided from the inner surface of the container. Therefore, the radial point at which the calculated scalar flux is selected for comparison with measurements is a radial position just inside the container on the reactor side of the assembly (See section A-A of fig. 3.) This corresponds to a radial position 4.4 cm less than that of the detector centerline.

Power Calibration

In order to compare the calculated results with the experimental measurements on absolute basis, both were normalized to correspond to a reactor thermal power level of 1 watt. For the calculated results this was done by assuming 2.43 neutrons produced per fission and 3.3×10^{10} fission per second per watt.

The reactor power was calibrated by mapping thermal flux in the reactor with dysprosium foils which had been previously calibrated against gold foils. The total fission rate was then calculated and correlated with readings on the reactor-control B^{10} ion chambers to obtain reactor power levels for all other measurements. The uncertainty in the absolute power levels is estimated to be ±10 percent.

CALCULATIONS

The flux per unit energy in the three experimental configurations (no intermediate lead wall, 5 and 10 cm lead wall) were calculated using the one-and two-dimensional discrete ordinates codes ANISN and DOT. The spatial distribution of the source used was that calculated from a two-dimensional reactivity-calculation for the reactor/lead/water configuration. In all cases, an S_8 angular quadrature and P_3 scattering approximation were used. Cross sections were from the libraries of GAM-II.

Tests of two cross section sets with different energy group splits were made with ANISN calculations to determine the adequacy of the fewer group set used in two-dimensional DOT calculations, as well as, subsequent ANISN calculations. ANISN and DOT calculations were made with identical cross sections and radial geometry. Differences between these calculation could then be attributed to deficiencies in the calculation (estimation) of transverse leakage in the one-dimensional calculation.

Analytic Model of Experiment

Geometry. - The geometry model of the experiment used in the calculations is shown in figure 1. The 25.4 cm diameter by 50.8 cm high cylindrical UO_2F_2/H_2O solution reactor is contained by a type-316 stainless steel vessel 0.278 cm thick by 91.4 cm high. The 20.3 cm thick $\times$ 91.4 cm high lead annulus then surrounds the reactor core. The remaining volume (to 121.5 cm radius) contains water with or without a 5- or 10-cm thick intermediate lead wall in place.

The following number of spatial mesh intervals were used in the one dimensional (cylindrical) calculations: 15 in the reactor core, two each in the steel vessel and small water region, and 25 in the 20.3 cm lead region. In the remaining water region (and intermediate lead wall region, if present)

a spatial mesh width of 1 cm was used. For the two-dimensional r-z cylindrical calculations, the following spatial mesh was used: axially, 27 intervals were more or less uniformly spaced (because of symmetry, only the half-geometry of figure 1 was calculated); radially, 11 intervals were used in the core, two each in the steel vessel and small water region, 15 in the 20.3 cm lead region. In the remaining water region (and intermediate lead wall region if present), a radial spatial mesh ranging in width from 1.0 to 3.0 cm was used. A total of 35 mesh points were used in this remaining region. Altogether, then, 65 mesh intervals were used in the radial direction in the two-dimensional transport calculations.

Material. - The atom densities for each region in the calculation are listed in table I. The critical fuel solution corresponds to a hydrogen-to-U-235 atom ratio of 641.

Sensitivity to Number of Energy Groups

To minimize computer time on the transport calculations, one would like to minimize the number of energy groups used but not jeopardize the accuracy of the calculation. To this end, identical one-dimensional calculations were made using two energy group structures. For this particular test, the configuration considered was that with the 10 cm thick intermediate lead wall placed in the water tank. The two group splits considered are listed in table II. They will hereafter be referred to as the fine group split and broad group split. The calculations reported here extend from 0.9 to 15 MeV, corresponding to the effective energy range of the neutron spectrometer. The multigroup cross sections were calculated using the GAM-II libraries and code.

The one dimensional cylindrical transport calculations were performed using an S_8 angular quadrature and P_3 scattering approximation. Transverse (axial) leakage rate was calculated by energy group and space point

in the calculation using a "leakage" cross section equal to DB^2. The "buckling" B was taken to be $\pi/(H + 2 \times 0.71\,\lambda_{TR})$, H is the height of the assembly (91.5 cm) and λ_{TR} is equal to $1/\Sigma_{TR}$, where Σ_{TR} is the transport cross section. Σ_{TR} is calculated from the recipe

$$\Sigma_{TR} = \Sigma_T - \overline{\mu}\Sigma_s$$

where Σ_T is the total cross section and Σ_s is the scattering cross section. μ is calculated from the total P_o and P_1 scattering cross sections in the GAM libraries by energy group. That is,

$$\overline{\mu} = \frac{\Sigma_s^1}{\Sigma_s^o}$$

Finally the diffusion coefficient D is $1/3\,\Sigma_{TR}$ and

$$DB^2 = \left(\frac{\lambda_{TR}}{3}\right)\left(\frac{\pi}{H + 2 \times 0.71\,\lambda_{TR}}\right)^2$$

This "buckling" or "leakage" cross section is added to Σ_T in the course of running the one-dimensional calculation.

The neutron energy spectrum as calculated with the two group splits of table II is shown in figure 4. Shown here is the energy spectrum calculated at three points in the assembly; these points are at radii 43 cm, 76 cm, and 100 cm (see fig. 1) and are within the range of the measurements taken. The point to be made here is that the results calculated here reflect only the differences in the group split; the conclusion to be drawn from this set of curves is that the fine energy group split and the broad energy group split give essentially the same results, even to a depth of 100 cm.

Comparison of One- and Two-Dimensional Calculations

Criticality calculations of this reactor/lead/water configuration showed that the critical height and/or uranium concentration could not be predicted by a one dimensional calculation. The "chimney" of lead rising above and below the reactor solution level provided enough returning neutrons to make the problem two-dimensional. A two-dimensional cylindrical r-z calculation was necessary to determine the proper eigenvalue. The fission density in the core, F(r, z) was not found to be separable in the two principle directions. That is

$$F(r, z) \neq R(r)\ Z(z)$$

In spite of this, it was believed that, away from the core, one-dimensional calculations of this configuration should give results comparable to two-dimensional results on the midplane of the assembly. This, of course, is the result of predominantly forward transmission of high (6-15 MeV) energy neutrons and a local slowing down spectrum determined by the magnitude of the high energy flux. This premise was tested.

Two dimensional r-z calculations were made for the three experimental configurations, water only in the outboard region, water plus a 5 cm Pb wall, and water plus a 10 cm Pb wall. S_8 angular quadrature and P_3 scattering approximation were used. The broad group energy split of table II was used. Based on the results of the previous section, this should introduce no error into the calculation. The spatial mesh was described earlier in this report. The source spatial distribution was that calculated from the criticality calculation and had a fission spectrum.

Neutron energy flux spectrum as calculated by the one- and two-dimensional transport codes at several points is shown in figure 5. The spectra shown here are for the case with the 10 cm intermediate lead wall in place. Results from other cases are similar. The spectra are shown for radial positions of 43.5, 76, and 100 cm. The spectra are normalized to a source strength of 2 neutrons/sec in the reactor core. Both one- and two-dimensional calculations were done with 13 energy groups (table II) to permit an easy comparison. Differences will be due primarily to the ap-

proximations in the one-dimensional calculation in calculating transverse leakage.

The results shown in figure 5 show that at the 43.5 cm position, the spectrum (from one- and two-dimensional calculations) are virtually identical on an absolute basis above 8 MeV; below this there is up to a 10 percent difference with the one-dimensional calculation giving the lower value. At the 76 cm position the one-dimensional results are consistently higher than the two dimensional by about 15 percent. Finally at the 100 cm position, the one dimensional results are higher than the two dimensional results by 20 to 30 percent. Because the angular quadrature, scattering order, and cross sections used in both one- and two-dimensional calculations were identical, only the differences in mesh spacing and transverse leakage remain suspect.

Because the mesh spacing in the two-dimensional calculation is less than a total-mean-free path in all groups with energy greater than 1.35 MeV, this does not seem to be the source of the discrepancy. Generally though, from past experience a smaller mesh size has been observed to increase calculated neutron transmission but this was not explored further here. The sensitivity in the formulation of "transverse leakage cross section," DB^2 used in the one-dimensional calculations was examined. This was demonstrated by changing the term in the denominator of the DB^2 expression from $H + 2 \times 0.71 \times \lambda_{TR}$ to H (the extrapolated height of the system is replaced by the physical height of the system) and rerunning the calculation. This change has the effect of increasing the buckling and hence the transverse leakage. The flux at the 100 cm position was now in agreement with the two-dimensional results for energies above 4 MeV but was below them for energies below 4 MeV. The flux at the 43.5 cm position is now consistently below the two-dimensional results by 5 to 10 percent. Perhaps some formulation for a transverse leakage cross section can be devised which gives a consistent comparison of a one-dimensional calculation with its two-dimensional equivalent; but such a formulation will not be attempted here.

The conclusions of the cross-comparison of one- and two-dimensional results are that:

1. One-dimensional results give surprisingly good agreement with two-dimensional results (to within 25 to 30 percent at the 100 cm position, less at lesser distances from the source) when the "standard" formulation of transverse leakage is used.

2. Because of uncertainties and sensitivity in the semi-empirical "transverse leakage cross section" used in the one-dimensional case, more confidence is placed in the two-dimensional results.

Smoothing of Calculated Results

It is inaccurate to quantitatively compare a calculated multigroup histogram spectra with a continuous, measured spectra since the measured spectra is smeared by some resolution function of the instrument. In the present case, this resolution, expressed as the half width at half maximum of a gaussian distribution, amounts to more than 1/2 MeV at 14 MeV neutron energy and about 0.3 MeV at 2 MeV neutron energy. To facilitate comparisons with experiments, the calculated multigroup spectra were smeared by a gaussian distribution function with the above resolution. This operation is reasonable to do when the multigroup energy width is of the order of the resolution. In the present case several energy groups above 6 MeV have widths larger than the resolution of the instrument so that the resulting smoothed calculated spectra will have artificial plateaus but with smooth corners. However, the resulting smooth curve is easier to compare with the experimental curve than the multigroup histogram. These plateaus are artificial and should disappear if a finer multigroup calculation were performed.

RESULTS

Multigroup scalar fluxes determined by the 13 group P_3S_8 two-dimensional transport calculations and smoothed by the gaussian smearing function were compared with measurements taken at several positions in each of three experimental configurations. These are shown in figure 6. Figure 6(a) shows the comparison for the case of water only in the region

outside of the 20.3 cm thick lead wall (see fig. 1 for orientation). Shown is the experimentally measured flux per unit energy, the calculated histogram multigroup flux per unit energy, and the smoothed histogram. All flux values are absolute and correspond to a reactor power level of 1 watt. Detector centerline positions are at radii of 54.3, 77.1, and 100 cm. The calculated fluxes at radii 49.9, 72.7, and 95.6 cm are assumed to correspond with the effective center of detection positions as discussed in a previous section. Figure 6(b) shows the comparison for the case of a 5 cm thick lead wall positioned in the outboard water region for a detector centerline position of 100 cm radius. Finally figure 6(c) shows the results for the case of a 10 cm thick lead wall positioned in the outboard water region; detector positions are at radii 79.6 cm (just outside of the 10 cm Pb wall) and at 100 cm. Again, the uniform shape agreement of measured and calculated fluxes at radii 4.4 cm less than the detector centerline positions confirm the assumed location of the effective center of detection of the detector assembly.

There is reasonable overall agreement between the calculated and experimental absolute flux spectra. In figure 6(a), the case with only water in the outboard region, agreement is within 30 percent at all energies and detector positions. This is probably within the reproducibility of the experiment considering the precision of determining absolute reactor power level, detector position, and possible variations in center of detection with neutron energy. Figure 6(a) shows the expected spectrum hardening with depth of penetration in water. It also shows a little of the oxygen scattering cross section structure at lower energies, but this is masked by the resolution of the instrument. A consistent shape difference appears to exist between the calculated and measured spectra; the calculated flux is consistently higher than the measurements for neutron energies above 4 to 6 MeV, and consistently lower for lower energies. Figures 6(b) and (c) show this same trend. This is not attributed to the lead cross sections because of the agreement between calculation and experiment at points near the lead (fig. 6(a), R = 54.3 cm; fig. 6(c), R = 79.6 cm). It may suggest that the water (oxygen) cross section is too low above 6 MeV.

Some other points of interest may be made by comparing the results at the 100 cm detector position for the three cases, no intermediate lead wall, 5 cm wall, and 10 cm wall (see figs. 6(a), (b), and (c), respectively). The 100 cm detector position is about 30 cm beyond the intermediate wall and is, of course, surrounded by water. The spectra for all three cases are reasonably identical in shape and magnitude. There is a consistent difference in spectral shape, however; that for the 10 cm thick lead wall has fewer 6 to 14 MeV neutrons and more 1 to 4 MeV neutrons than the water only case. The case for the 5 cm thick lead wall is in between the 10 cm lead case and the water case as expected. This is a result of neutron inelastic scattering events in the lead. The fact that the spectra are almost identical in magnitude is a coincidence of high energy inelastic scattering properties of MeV neutrons by lead being almost the same as elastic scattering properties of water.

This is again demonstrated by figure 6(c) which shows the spectra immediately following the 10 cm thick intermediate lead wall (detector position, 79.6 cm) and that at the 100 cm position, some 20 cm deeper into the water. The 79.6 cm position spectra shows the buildup of 1 to 3 MeV neutrons from inelastic scatter events in lead. The 100 cm position measurement shows the return to an equilibrium spectrum. The magnitude of the buildup of inelastically scattered neutrons may be seen more clearly by comparing the 79.6 cm position spectra of figure 6(c) and the 77.1 cm position of figure 6(a) (water only).

CONCLUDING REMARKS

Measurements of neutron spectra have been made in a cylindrical shield arrangement surrounding a small cylindrical shaped UO_2F_2-water solution reactor. The shield consisted of concentric layers of lead and water. Spectrum measurements were made with a NE-213 scintillation spectrometer immersed in the water region of the shield. Measurements were made along the reactor midplane to shield depths of 100 cm.

One-dimensional calculations made with two different energy group splits justified using the fewer group split in two-dimensional calculations.

Comparison of one- and two-dimensional calculations with the same cross sections showed a divergence of results for deeper penetrations. This was attributed to approximations used in determining transverse leakage in the one-dimensional calculations. Even at 100 cm depth, though, the one- and two-dimensional calculations differed by not more than about 30 percent. The one-dimensional results were consistently above the two-dimensional results.

Calculations of absolute neutron flux spectra made with the two-dimensional code DOT agree reasonably well with the experimental measurements in both magnitude and shape. There is a consistent difference in spectral shape, however; namely that the measured spectra was greater than that calculated for neutron energies below about 4 MeV, and vice versa for neutrons above 4 MeV. The cause of this is presently unknown and being investigated. The spectra show the expected hardening with depth of penetration as well as the same shape with and without an intermediate lead shield in place for deep penetrations.

REFERENCES

1. W. W. ENGLE, Jr., "A User's Manual for ANISN: A One-Dimensional Discrete Ordinates Transport Code with Anisotropic Scattering," K-1693, Union Carbide Corp. (March 20, 1967).
2. F. R. MYNATT, "A User's Manual for DOT: A Two-Dimensional Discrete Ordinates Transport Code with Anisotropic Scattering," K-1694, Union Carbide Corp. (1967).
3. R. G. SOLTESZ and R. K. DISNEY, "User's Manual for the DOT-IIW Discrete Ordinates Transport Computer Code," WANL-TME-1982, Westinghouse Astronuclear Laboratory (December 1969).
4. G. D. JOANOU and J. S. DUDEK, "GAM-II. A B_3 Code for the Calculation of Fast-Neutron Spectra and Associated Multigroup Constants," GA-4265, General Atomics Division, General Dynamics Corp. (September 16, 1963).

5. V. V. VERBINSKI, W. R. BURRUS, T. A. LOVE, W. ZOBEL, and H. W. HILL, "Calibration of an Organic Scintillator for Neutron Spectroscopy," Nucl. Inst. Methods, 65, 8 (1968).
6. W. R. BURRUS and V. V. VERBINSKI, "Fast-Neutron Spectroscopy with Thick Organic Scintillators," Nucl. Inst. Methods, 67, 181 (1969).
7. L. CLEMONS, Jr., G. N. WRIGHTS, and D. F. SHOOK, "Monte Carlo Calculations of a Hemispherical-Duct Neutron-Streaming Experiment," NASA TM X-1971 (1970).

TABLE I. - ATOM DENSITIES OF MATERIAL

USED IN CALCULATIONS

Region	Element or isotope	Atom density, 10^{24} atoms/cm^3
Reactor core ($H/U^{235} = 641$)	Hydrogen	0.066395
	Oxygen	.033420
	Fluorine	.00022236
	U-235	.00010363
	U-238	.00000755
Water	Hydrogen	0.067
	Oxygen	.0335
Stainless steel reactor tank	Chromium	0.015590
	Iron	.060638
	Nickel	.009745
Lead	Lead	0.033

TABLE II. - MULTIGROUP ENERGY BOUNDARIES

Group number	Energy group upper boundary, MeV	
	Fine group split	Broad group split
1	14.92	14.92
2	13.50	12.21
3	12.21	10.00
4	11.05	8.19
5	10.00	6.07
6	9.05	4.97
7	8.19	4.07
8	7.41	3.01
9	6.70	2.47
10	6.07	2.23
11	5.49	1.83
12	4.97	1.35
13	4.49	1.11
14	4.07	.91
15	3.68	
16	3.33	
17	3.01	
18	2.73	
19	2.47	
20	2.23	
21	2.02	
22	1.83	
23	1.65	
24	1.50	
25	1.35	
26	1.22	
27	1.11	
28	1.00	
29	.91	

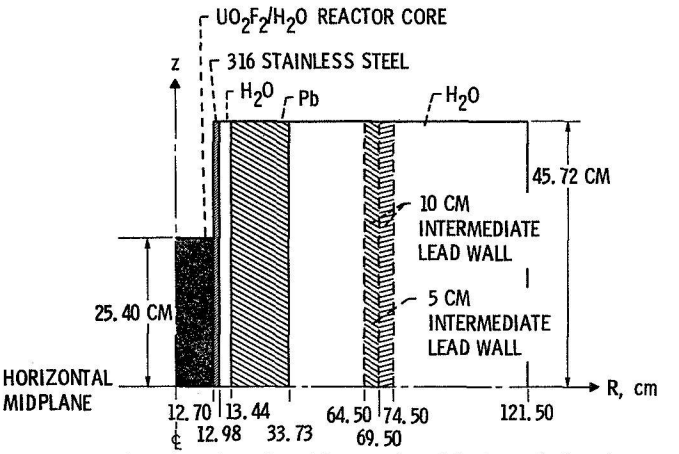

Figure 1. - Geometry of the experimental setup. Region above horizontal midplane is shown. The geometry is symmetric about the midplane.

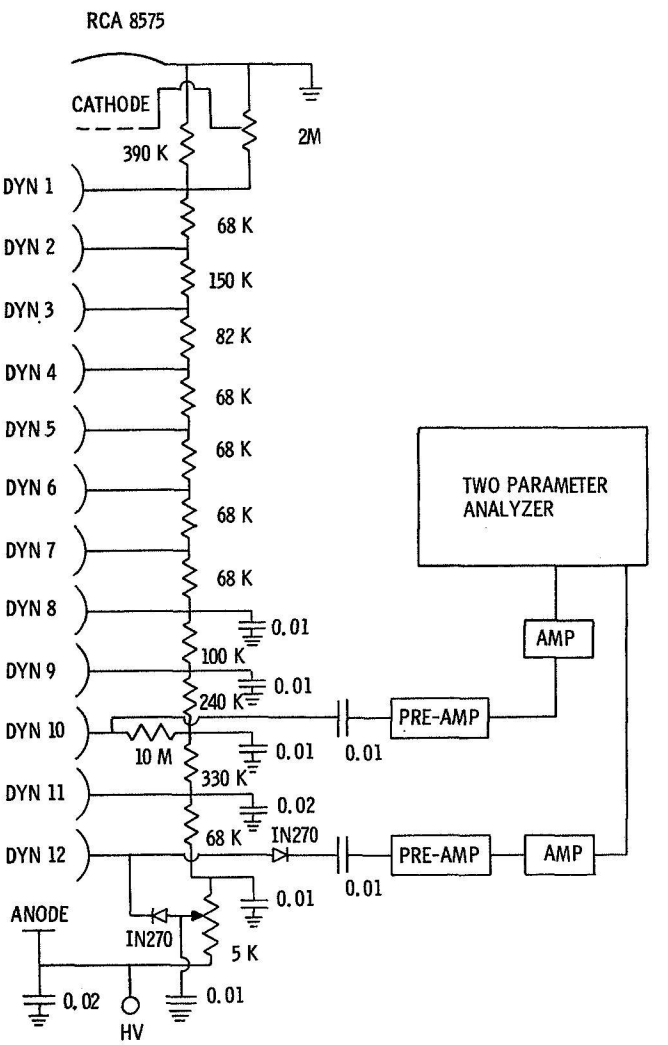

Figure 2. - Spectrometer block diagram and photomultiplier tube base circuit.

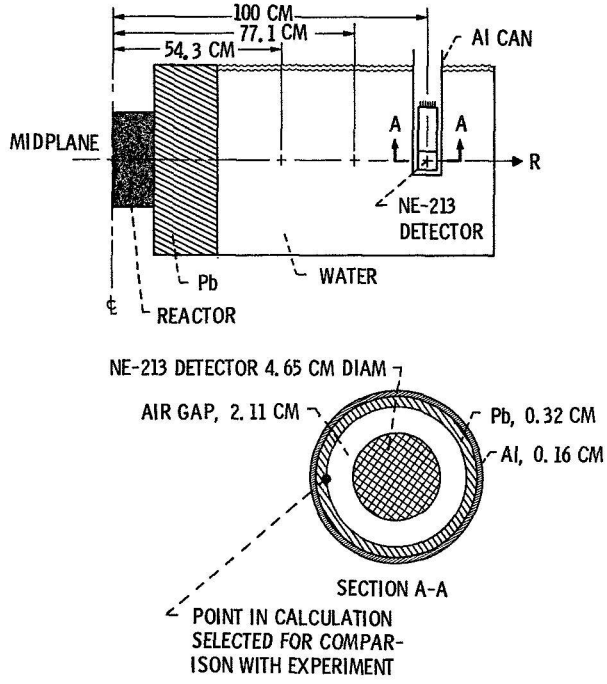

Figure 3. - Detector geometry within experimental assembly.

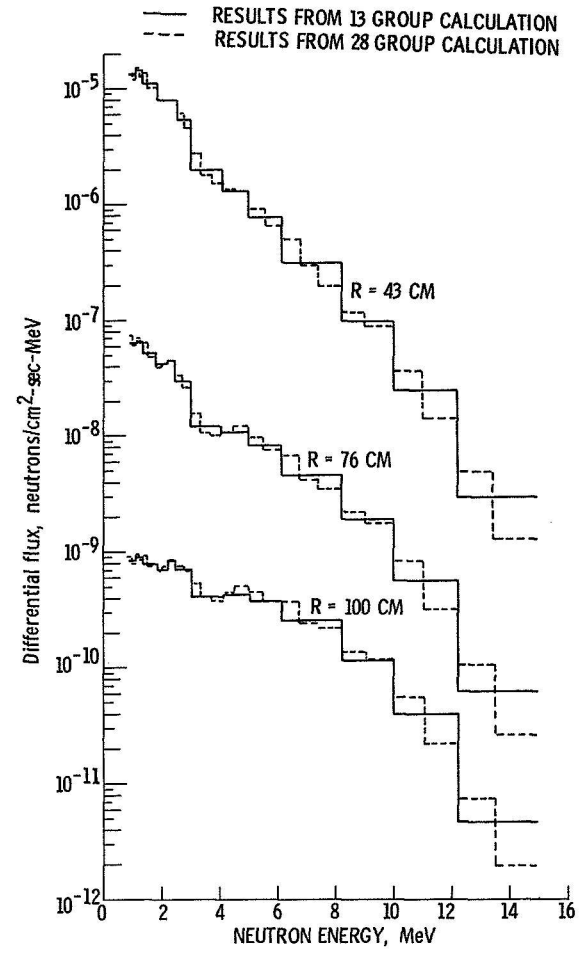

Figure 4. - Comparison of calculations with fine and coarse energy group splits. Neutron energy flux spectrum calculated at midplane of experiment for several radial positions. Source normalization is 1 neutron per cm of reactor height. One dimensional calculations made with 13- and 28 energy groups. Calculation shown is for case with 10 cm thick intermediate lead wall.

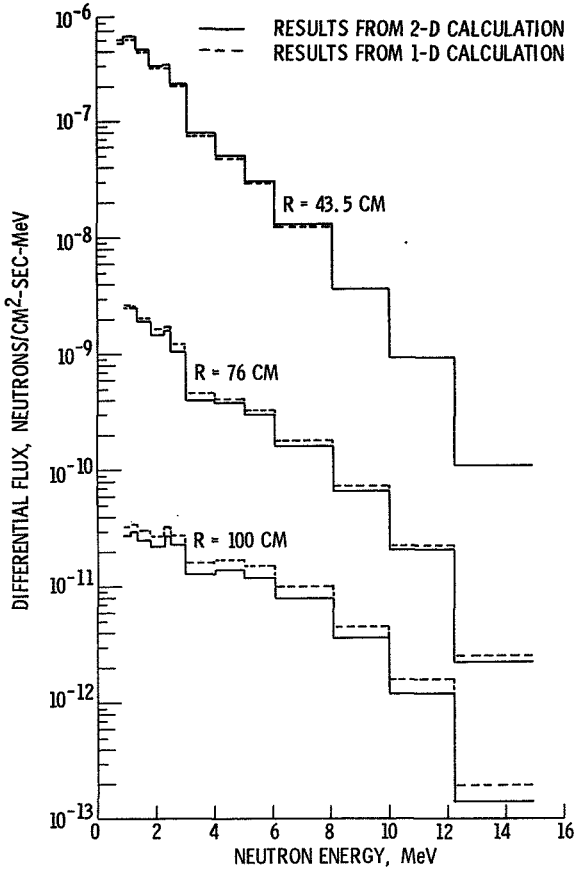

Figure 5. - Comparison of neutron spectra evaluated by one- and two-dimensional calculations. Neutron energy flux calculated at midplane of experiment for several radial positions. Source normalization is 2 neutrons per second born in reactor. Calculations made for the configuration with 10 cm thick intermediate lead wall.

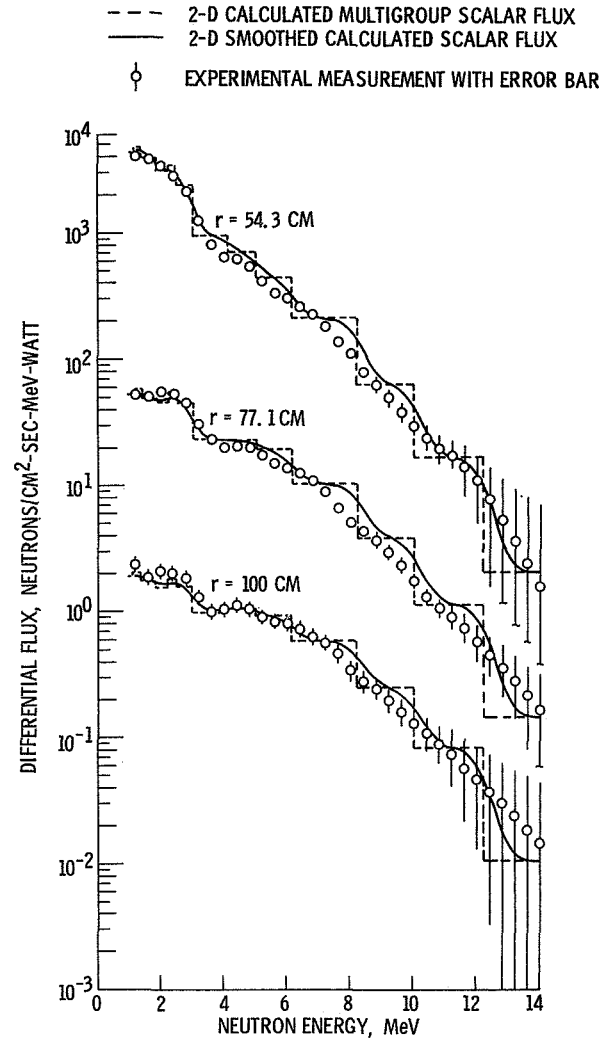

(A) COMPARISON FOR CASE WITH WATER ONLY IN OUTBOARD REGION.

Figure 6. - Comparison of calculated scalar flux, calculated scalar flux which has been smoothed, and experimental measurements. Calculations are results of two-dimensional transport calculations, 13 energy groups, S_8 angular quadrature and P_3 scattering.

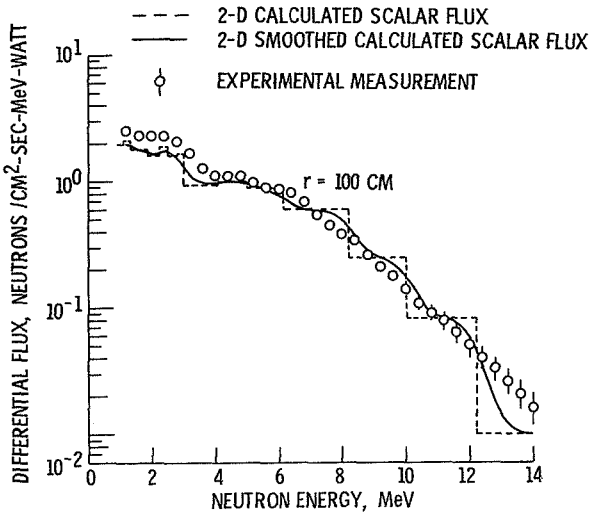

(B) COMPARISON FOR CASE WITH 5 CM INTERMEDIATE Pb WALL IN PLACE.

Figure 6. - Continued.

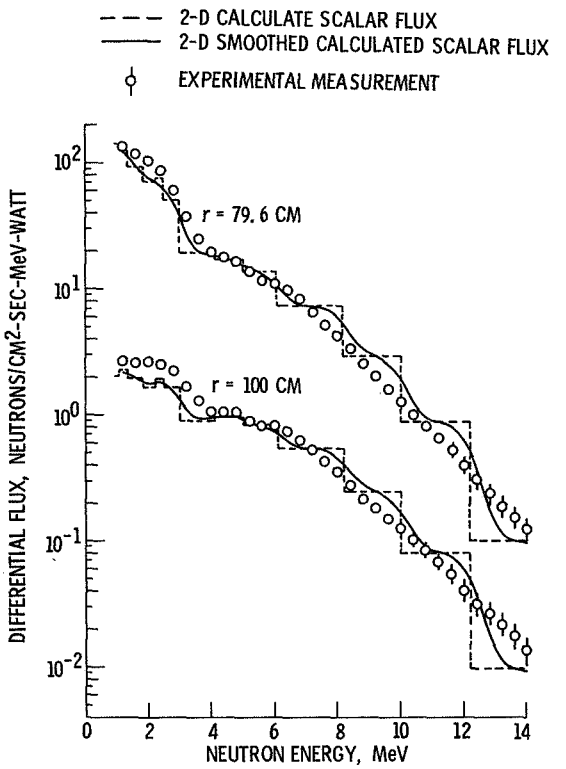

(C) COMPARISON FOR CASE WITH 10 CM INTERMEDIATE Pb WALL IN PLACE.

Figure 6. - Concluded.

NASA-Lewis-Com'l